Physics Letters A ••• (••••) •••–•••

Contents lists available at ScienceDirect

Physics Letters A

www.elsevier.com/locate/pla

First-principles calculations of the dielectric and vibrational properties of ferroelectric and paraelectric $BaAl_2O_4$

Congwei Xie [a], Qingfeng Zeng [a,*], Dong Dong [a], Shuang Gao [a], Yongqing Cai [b], Artem R. Oganov [c,d,e]

[a] Science and Technology on Thermostructural Composite Materials Laboratory, School of Materials Science and Engineering, Northwestern Polytechnical University, Xi'an, Shaanxi 710072, PR China
[b] Institute of High Performance Computing, 1 Fusionopolis Way, Singapore 138632, Singapore
[c] Department of Geosciences, Center for Materials by Design, and Institute for Advanced Computational Science, State University of New York, Stony Brook, NY 11794-2100, USA
[d] Moscow Institute of Physics and Technology, Dolgoprudny, Moscow Region 141700, Russia
[e] School of Materials Science and Engineering, Northwestern Polytechnical University, Xi'an, Shaanxi 710072, PR China

ARTICLE INFO

Article history:
Received 12 December 2013
Received in revised form 17 April 2014
Accepted 24 April 2014
Available online xxxx
Communicated by R. Wu

Keywords:
First-principles
Dielectric properties
$BaAl_2O_4$ polymorphs
Transparent materials

ABSTRACT

First-principles calculations have been conducted to study the structural, dielectric, and vibrational properties of ferroelectric and paraelectric $BaAl_2O_4$. High-frequency and static dielectric constants, and phonon frequencies at the Brillouin zone center are reported. Both $BaAl_2O_4$ polymorphs are promising infrared-transparent materials due to their low electronic dielectric constants. The ferroelectric and paraelectric $BaAl_2O_4$ have much smaller permittivity compared to the classical ferroelectric materials. From an atomic nanostructure standpoint, the abnormally low permittivity of $BaAl_2O_4$ polymorphs is mainly related to low coordination numbers of Ba (9) and Al (4).

1. Introduction

$BaAl_2O_4$ has attracted a great attention due to its intriguing optical properties and exciton effect evidenced by strong photoluminescence emission [1,2]. This material also shows excellent dielectric and pyroelectric properties. However, as a typical complex oxide, $BaAl_2O_4$ has a much smaller dielectric constant than classical ferroelectric materials like $BaTiO_3$ (average static dielectric constant can reach 2450 [3]). The origin of this unexpectedly low dielectric constant of $BaAl_2O_4$ is still unclear. Understanding the polarization mechanism and ionic contribution to the dielectric constant is critically important for its optoelectronic applications.

$BaAl_2O_4$ exhibits a paraelectric–ferroelectric (PE–FE) phase transition over a wide temperature range (400–670 K) [4]. In both structures, corner-sharing AlO_4 tetrahedra form a three-dimensional network with hexagonal channels which are filled with Ba^{2+} cations [4,5]. The crystal structure of low-temperature FE phase has been determined by single-crystal [6] and powder [7] X-ray diffraction, respectively. The FE phase adopts a hexagonal structure (space group $P6_3$) [6,7]. The crystal structure of the PE phase was proposed by Huang et al. [7], who suggested that PE phase has a $P6_322$ symmetry, which was confirmed by high resolution electron microscopy study performed by Abakumov et al. [4].

First-principles calculations are capable of predicting the material properties using no empirical data, and this gives the promise to speed up materials research [8,9]. This work aims to investigate the dielectric and vibrational properties of $BaAl_2O_4$ polymorphs using first-principles calculations. The crystal structures of FE and PE phases in this study are from the data of Huang et al. [7] and Abakumov et al. [4], respectively.

2. Computational methodology

The present first-principles calculations were carried out using the CASTEP code [10] with norm-conserving pseudopotentials [11]. Modified Perdew–Burke–Ernzerhof GGA functional for solids (PBEsol) [12] was applied to describe the exchange and correlation potentials. The kinetic energy cutoff for the plane waves was 900 eV. To sample the Brillouin-zones, a $2 \times 2 \times 2$ ($5 \times 5 \times 3$) Monkhorst–Pack grid of k-points [13] was adopted for a primitive cell of FE phase (PE phase). The convergence tolerance of energy change, maximum force on each atom and stress of the optimized

* Corresponding author. Tel.: +86 29 88495619; fax: +86 29 88494620.
E-mail address: qfzeng@nwpu.edu.cn (Q. Zeng).

http://dx.doi.org/10.1016/j.physleta.2014.04.047
0375-9601/

Table 1
Optimized lattice constants and the internal atom coordinates of the FE-$BaAl_2O_4$ and PE-$BaAl_2O_4$.

Compound	Space group (No.)	Lattice constants (Å)	Atom position (Wyckoff position)
FE-$BaAl_2O_4$	$P6_3$ (173)	$a = 10.264$ $c = 8.656$ $a = 10.449$ [7] $c = 8.793$ [7] $a = 10.369$ [1] $c = 8.807$ [1]	Ba1(2a) (0, 0, 0.247) Ba2(6c) (0.506, 0.005, 0.258) Al1(6c) (0.157, 0.332, 0.063) Al2(6c) (0.155, 0.329, 0.451) Al3(2b) (1/3, 2/3, 0.947) Al4(2b) (1/3, 2/3, 0.550) O1(6c) (0.180, −0.002, 0.984) O2(6c) (0.686, −0.001, 0.039) O3(6c) (0.497, 0.184, −0.006) O4(6c) (0.181, 0.501, 1.002) O5(6c) (0.121, 0.324, 0.257) O6(2b) (1/3, 2/3, 0.749)
PE-$BaAl_2O_4$	$P6_322$ (182)	$a = 5.113$ $c = 8.730$ $a = 5.224$ [4] $c = 8.793$ [4]	Ba(2b) (0, 0, 1/4) Al(4f) (1/3, 2/3, 0.054) O1(6g) (0.359, 0, 0) O2(2c) (1/3, 2/3, 1/4)

structure was 1×10^{-5} eV/atom, 0.01 eV/Å, and 0.05 GPa, respectively.

The calculation of vibrational and dielectric properties were performed using density functional perturbation theory (DFPT) [14]. Γ-phonon frequencies and dielectric tensors were computed as second derivatives of the total energy with respect to atomic displacements or external electric field [15,16]. The longitudinal-optical/transverse-optical (LO/TO) splitting of zone center optical modes was investigated parallel and perpendicular to the (001) direction approaching to Γ-point.

3. Results and discussions

3.1. Structure optimization

The crystal structure of FE-$BaAl_2O_4$, containing 56 atoms in its unit cell, is a hexagonal structure with space group $P6_3$. Figs. 1a and 1b represent b–c and a–b plane of the unit cell, respectively. Three-dimensional tridymite-like framework is made of AlO_4 tetrahedra with Ba atoms situated in the hexagonal channels. The structure of the FE-$BaAl_2O_4$ contains four symmetrically inequivalent Al atoms with clearly distinct coordination environment (Fig. 1c). Both the $(Al3)O_4$ tetrahedron and $(Al4)O_4$ tetrahedron have a three-fold symmetry axis, and the two tetrahedra share the same oxygen atom (O6). The (Al3)–(O6)–(Al4) bond angle is 180°. At the same time, the $(Al1)O_4$ and $(Al2)O_4$ tetrahedra are distorted, and the (Al1)–(O5)–(Al2) bond angle is 155.3°. Figs. 2a and 2b show that the b–c and a–b plane of the $2 \times 2 \times 1$ superstructure of PE-$BaAl_2O_4$, respectively. PE- and FE-$BaAl_2O_4$ display group–subgroup relations: their structural topology is the same, with the FE phase being symmetry-broken. FE-$BaAl_2O_4$ also has a larger cell (a $2 \times 2 \times 1$ supercell of PE-$BaAl_2O_4$). All Ba atoms in PE-$BaAl_2O_4$ are symmetrically equivalent. All Al atoms in PE-$BaAl_2O_4$ are also symmetrically equivalent and the (Al)–(O2)–(Al) bond angle is 180° (Fig. 2c).

Computed structural parameters of both phases are listed in Table 1 and values from other reports are also listed for comparison. Our calculated lattice constants of FE-$BaAl_2O_4$ are close to the experimental results [7] and other calculated results obtained by using GGA-PBE [1]. The present structural parameters of PE-$BaAl_2O_4$ are also comparable to the experimental results [4].

3.2. Electronic dielectric constants

Due to the anisotropic hexagonal symmetry of the $BaAl_2O_4$, the calculated dielectric tensor has two independent components

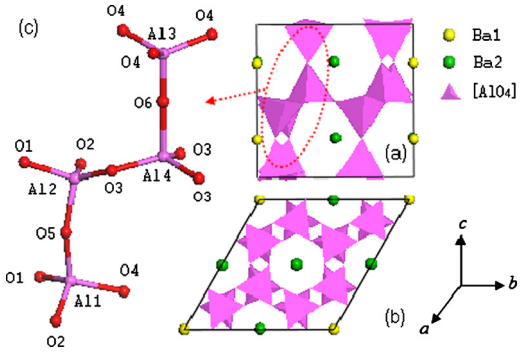

Fig. 1. Crystal structure of FE-$BaAl_2O_4$: (a) b–c plane of the unit cell, (b) a–b plane of the unit cell, and (c) coordination environments of Al atoms in the FE-$BaAl_2O_4$.

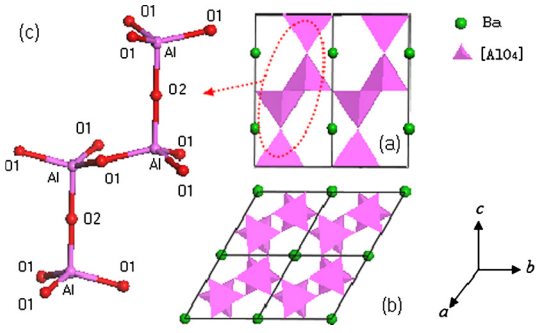

Fig. 2. Crystal structure of PE-$BaAl_2O_4$: (a) b–c plane of the $2 \times 2 \times 1$ supercell, (b) a–b plane of the $2 \times 2 \times 1$ supercell, and (c) coordination environments of Al atoms in the PE-$BaAl_2O_4$.

$\varepsilon_{\perp c}$ and $\varepsilon_{\parallel c}$ (perpendicular to and parallel to the c axis). Our present values of the electronic dielectric constants are $\varepsilon_{\infty,\perp c} = 3.12$ and $\varepsilon_{\infty,\parallel c} = 3.13$ for FE-$BaAl_2O_4$. The average permittivity $\bar{\varepsilon}_\infty$, obtained from the expression $\bar{\varepsilon}_\infty = (2\varepsilon_{\infty,\perp c} + \varepsilon_{\infty,\parallel c})/3$, is 3.12. The calculated values of $\varepsilon_{\infty,\perp c}$, $\varepsilon_{\infty,\parallel c}$ and $\bar{\varepsilon}_\infty$ for PE-$BaAl_2O_4$ are 3.12, 3.14 and 3.13, respectively, which are similar to those of FE-$BaAl_2O_4$.

Using the electronic dielectric constants, we can obtain some other properties such as the index of refraction n, the reflectivity R, and the optical transmittance T. These properties can also help us to confirm the accuracy of our calculations. For nonmagnetic materials, the index of refraction n and reflectivity R of $BaAl_2O_4$ can be calculated by $n = \varepsilon^{1/2}$ and $R = (n-1)^2/(n+1)^2$, respectively.

Table 2
Electronic dielectric constants, the index of refraction and transmittance of $BaAl_2O_4$ polymorphs.

Compound	$\varepsilon_{\infty,\perp c}$	$\varepsilon_{\infty,\parallel c}$	$n_{\infty,\parallel c}$	T
FE-$BaAl_2O_4$	3.12	3.13	1.77	92.3%
			1.74 ± 0.03 [7]	93.0% [1]
PE-$BaAl_2O_4$	3.12	3.14	1.77	92.3%

The optical transmittance T of $BaAl_2O_4$ is equal to $(1-R)$ assuming without optical absorption.

Electronic polarization mainly contributes to the light absorption in the UV region, while ionic polarization plays a major part in the infrared region. It was reported that $BaAl_2O_4$ has a very low absorption and no absorption peak in the wavelength range from 200 nm to 2500 nm [1], which suggested that total polarization almost stays constant in this UV to near-IR (NIR) region. Thus, the dielectric permittivity of the $BaAl_2O_4$ has very small variation in this wavelength range. We can utilize the calculated ε_∞ to obtain some properties in UV-NIR region, not rigorously but effectively. These results are listed in Table 2. Our theoretical value of $n_{\parallel c}$ of FE-$BaAl_2O_4$ is 1.77 which agrees well with experimental data 1.74 ± 0.03 measured at 543 nm using a single crystal [7]. The optical transmittance of the FE-$BaAl_2O_4$ is 92.3% (93.0% from experiment [1]). For PE-$BaAl_2O_4$, the calculated optical transmittance is comparable to that of FE-$BaAl_2O_4$. Our study indicates both phases are UV-NIR wave-transparent materials due to their low electronic dielectric constants.

3.3. Phonons and static dielectric constants

Since the primitive unit cell of the FE-$BaAl_2O_4$ contains 56 atoms, there are a total of 168 vibrational modes, of which three are acoustic modes and the remaining 165 are optical ones. At the same time, PE-$BaAl_2O_4$ has 14 atoms in its primitive unit cell and there are a total of 42 modes, of which three are acoustic modes and the remaining 39 are optical ones. According to group theory [17], the irreducible representations of optical phonon modes at the Brillouin zone center are:

$$\Gamma_{optic} = 27A(\mathrm{IR,R}) + 27E_1(\mathrm{IR,R}) + 28B(\mathrm{S}) + 28E_2(\mathrm{R})$$

and

$$\Gamma_{optic} = 2A_1(\mathrm{R}) + 4A_2(\mathrm{IR}) + 3B_1(\mathrm{S}) + 4B_2(\mathrm{S}) + 6E_1(\mathrm{IR,R}) + 7E_2(\mathrm{R})$$

for FE-$BaAl_2O_4$ and PE-$BaAl_2O_4$, respectively. Where (IR) stands for IR-active, (R) for Raman-active, and (S) for silent; A, A_1, A_2, B, B_1 and B_2 are single degenerate mode, E_1 and E_2 are twofold degenerate modes.

For FE-$BaAl_2O_4$, inclusion of the long range polarization interaction results in the splitting of A and E_1 TO modes into corresponding LO modes, which gives 54 polar vibrations (27 A modes along c axis and 27 E_1 modes perpendicular to c axis). At the same time, for PE-$BaAl_2O_4$, 10 polar vibrations ($4A_2$ modes along c axis and $6E_1$ modes perpendicular to c axis) are given due to the LO/TO splitting of the A_2 and E_1 modes. As a result, different numbers of IR modes are active for $E_{\parallel c}$ and $E_{\perp c}$. Calculated values of the IR-active optical phonon frequencies are given in Tables 3 and 4. They are utilized to obtain static dielectric constants and the contribution of each IR-active mode to the lattice dielectric constants.

To obtain static dielectric constants, we applied the well-known generalized Lyddane–Sachs–Teller (LST) relationship [18]:

$$\varepsilon_0 = \varepsilon_\infty \prod_m \frac{\omega_{\mathrm{LO},m}^2}{\omega_{\mathrm{TO},m}^2} \tag{1}$$

Table 3
Vibrational properties of FE-$BaAl_2O_4$: phonon frequencies of IR-active modes and their contributions to the static dielectric constants.

$E_{\perp c}$				$E_{\parallel c}$			
Mode	ω_{TO}	ω_{LO}	ε_m^{lat}	Mode	ω_{TO}	ω_{LO}	ε_m^{lat}
E_1	63	68	1.39	A	63	63	0
	85	87	0.38		77	77	0
	93	94	0.17		79	79	0
	107	110	0.42		111	118	1.27
	123	132	0.98		121	147	3.16
	139	146	0.61		147	173	1.84
	162	183	1.27		200	200	0
	211	212	0.04		225	225	0
	240	241	0.04		259	259	0
	263	263	0		284	284	0
	287	287	0		345	345	0
	300	300	0		379	380	0.03
	370	371	0.02		395	395	0
	376	376	0		409	409	0
	412	416	0.09		413	452	0.79
	424	430	0.12		452	478	0.42
	437	464	0.48		561	561	0
	510	511	0.02		578	578	0
	688	688	0		666	666	0
	698	699	0.01		728	729	0.01
	742	760	0.18		802	804	0.02
	773	785	0.11		971	982	0.08
	1015	1019	0.03		1024	1024	0
	1024	1033	0.06		1048	1049	0.01
	1061	1078	0.11		1067	1072	0.03
	1087	1099	0.07		1082	1095	0.08
	1101	1119	0.10		1103	1138	0.20

Table 4
Vibrational properties of PE-$BaAl_2O_4$: phonon frequencies of IR-active modes and their contributions to the static dielectric constants.

$E_{\perp c}$				$E_{\parallel c}$			
Mode	ω_{TO}	ω_{LO}	ε_m^{lat}	Mode	ω_{TO}	ω_{LO}	ε_m^{lat}
E_1	92	110	3.19	A_2	109	172	7.14
	133	171	2.93		409	482	1.34
	363	367	0.10		978	983	0.04
	424	457	0.61		1121	1169	0.28
	744	775	0.30				
	1043	1102	0.36				

where $\omega_{\mathrm{TO},m}$ is the transverse optical mode frequency, and $\omega_{\mathrm{LO},m}$ the longitudinal optical mode frequency.

For FE-$BaAl_2O_4$, the static constants $\varepsilon_{0,\perp c}$ and $\varepsilon_{0,\parallel c}$ calculated by LST model are 9.82 and 11.09, respectively. The calculated average static dielectric constant (10.24) agrees with the experimental value (10.7 [19]) quite well. Huang et al. also reported the dielectric constant of FE-$BaAl_2O_4$ with a fractional porosity of 11% [20]. Their value is 7.50, which is different from our calculation. However, the effect of porosity on the dielectric properties should be considered. To obtain the average static dielectric constant of a porous media, we apply an empirical model derived by Maxwell [21]:

$$\varepsilon = \varepsilon_{matrix}\left(1 - \frac{3P(\varepsilon_{matrix} - 1)}{2\varepsilon_{matrix} + 1 - P + P\varepsilon_{matrix}}\right) \tag{2}$$

where P is the fractional porosity, ε_{matrix} the static dielectric constant of the matrix, and ε the static dielectric constant of the mixture. We obtain a theoretical static dielectric constant value of 8.85 for porous FE-$BaAl_2O_4$. This value agrees with Huang's data well.

Our calculated average static dielectric constant for PE-$BaAl_2O_4$ is 11.32, which is higher than that of FE-$BaAl_2O_4$ (10.24). We performed a deeper analysis of the contribution of each IR-active mode to the dielectric constant:

$$\varepsilon_m^{lat} = \begin{cases} \varepsilon_\infty\left(\prod_m \frac{\omega_{LO,m}^2}{\omega_{TO,m}^2} - \prod_{m-1} \frac{\omega_{LO,m-1}^2}{\omega_{TO,m-1}^2}\right) & (m > 1) \\ \varepsilon_\infty\left(\frac{\omega_{LO,1}^2}{\omega_{TO,1}^2} - 1\right) & (m = 1) \end{cases} \quad (3)$$

These values are also listed in Tables 3 and 4. It is easily found that the large contributions to lattice dielectric constants mainly come from the low-frequency modes. For FE-$BaAl_2O_4$, the modes at 63 cm^{-1} and 121 cm^{-1} makes the largest contributions to $\varepsilon_{0,\perp c}$ and $\varepsilon_{0,\parallel c}$, respectively. While for PE-$BaAl_2O_4$, the modes making the largest contributions to static constant perpendicular and parallel to (001) direction are 92 cm^{-1} and 109 cm^{-1}, respectively.

We can see that the static dielectric constants of the two $BaAl_2O_4$ phases are much smaller than that of classical ferroelectric materials like $BaTiO_3$ (average static dielectric constant can reach 2450 [3]). $BaTiO_3$ has one IR-active mode (12 cm^{-1}), a nearly soft mode that can result in a great value of $\omega_{LO,m}^2/\omega_{TO,m}^2$ (several hundred). For $BaAl_2O_4$, we do not see any nearly as soft phonons and no IR-active mode has such large effect on the dielectric constant (see $\omega_{TO,m}$ and $\omega_{LO,m}$ listed in Tables 3 and 4). We explain this by the anomalously low coordination numbers of Ba (9, instead of the more usual 12) and Al (4, instead of the more usual 6). The conclusion we draw is based on the relationship between atomic nanostructure and permittivity proposed by Rignanese et al. [22]. As a rule, the higher coordination numbers, the lower force constant and the higher dielectric constants. Such simple principles can help rational design of novel dielectric materials. The USPEX code [23,24] for crystal structure prediction may help us realize this idea in our future research work.

4. Conclusions

In summary, DFT and DFPT were used to investigate structural, vibrational, and dielectric properties of FE-$BaAl_2O_4$ and PE-$BaAl_2O_4$. Their high optical transmittances (>92.0%) obtained from the electronic dielectric constant indicate they are UV-NIR transparent materials. By the use of the well-known generalized LST relationship, we obtained the static dielectric constants of both $BaAl_2O_4$ polymorphs. The average static dielectric constant is slightly larger after the FE-PE transition (changing from 10.24 to 11.32). Further vibrational analysis shows that the large vibrational contributions to the lattice dielectric constants of the two phases mainly come from their low-frequency IR-active modes. Our theoretical results, in agreement with the experimental data well, confirm that $BaAl_2O_4$ polymorphs have very low dielectric permittivities compared with classical ferroelectric materials like $BaTiO_3$ (>2000). Their relatively low permittivities are due to low coordination numbers of Al and Ba, and the first-order FE-PE phase transition, which does not involve complete mode softening.

Acknowledgements

This work is supported by the Basic Research Foundation of NWPU (No. JCY20130114), National Natural Science Foundation of China (Nos. 51372203, 51332004), and Foreign Talents Introduction and Academic Exchange Program of China (No. B08040). The authors also acknowledge the High Performance Computing Center of NWPU for the allocation of computing time on their machines.

References

[1] L. Zhang, L. Wang, Y. Zhu, Adv. Funct. Mater. 17 (2007) 3781.
[2] M.V.S. Rezende, P.J. Montes, M.E.G. Valerio, R.A. Jackson, Opt. Mater. 34 (2012) 1434.
[3] K.F. Young, H.P.R. Frederikse, J. Phys. Chem. Ref. Data 2 (1973) 313.
[4] A.M. Abakumov, O.I. Lebedev, L. Nistor, G.V. Tendeloo, S. Amelinckx, Phase Transit. 71 (2000) 143.
[5] H.T. Stokes, C. Sadate, D.M. Hatch, L.L. Boyer, M.J. Mehl, Phys. Rev. B 65 (2002) 064105.
[6] V.W. Hörkner, H. Müller-Buschbaum, Z. Anorg. Allg. Chem. 451 (1979) 40.
[7] S. Huang, R. Von der Mühll, J. Ravez, M. Couzi, Ferroelectrics 159 (1994) 127.
[8] P.K. Mukherjee, Phys. Lett. A 377 (2013) 2436.
[9] Q. Zeng, L. Zhang, X. Zhang, Q. Chen, Z. Feng, Y. Cai, L. Cheng, Z. Weng, Phys. Lett. A 375 (2011) 3521.
[10] S.J. Clark, M.D. Segall, C.J. Pickard, P.J. Hasnip, M.I.J. Probert, K. Refson, M.C. Payne, Z. Kristallogr. 220 (2005) 567.
[11] D.R. Hamann, M. Schlüter, C. Chiang, Phys. Rev. Lett. 43 (1979) 1494.
[12] J.P. Perdew, A. Ruzsinszky, G.I. Csonka, O.A. Vydrov, G.E. Scuseria, L.A. Constantin, X. Zhou, K. Burke, Phys. Rev. Lett. 100 (2008) 136406.
[13] J.D. Pack, H.J. Monkhorst, Phys. Rev. B 16 (1977) 1748.
[14] S. Baroni, S. de Gironcoli, A.D. Corso, P. Giannozzi, Rev. Mod. Phys. 73 (2001) 515.
[15] X. Gonze, Phys. Rev. B 55 (1997) 10337.
[16] X. Gonze, C. Lee, Phys. Rev. B 55 (1997) 10355.
[17] A.M. Hofmeister, A. Chopelas, Phys. Chem. Miner. 17 (1991) 503.
[18] W. Cochran, R.A. Cowley, J. Phys. Chem. Solids 23 (1962) 447.
[19] A.A. Bush, A.G. Laptev, Fiz. Tverd. Tela 31 (1989) 317.
[20] S. Huang, R.V.D. Mühll, J. Ravez, J.P. Chaminade, P. Hagenmuller, M. Couzi, J. Solid State Chem. 109 (1994) 97.
[21] W.D. Kingery, H.K. Bowen, D.R. Uhlmann, Introduction to Ceramics, second edition, Wiley, New York, 1976.
[22] G.M. Rignanese, F. Detraux, X. Gonze, A. Bongiorno, A. Pasquarello, Phys. Rev. Lett. 89 (2002) 117601.
[23] A.R. Oganov, C.W. Glass, J. Chem. Phys. 124 (2006) 244704.
[24] C.W. Glass, A.R. Oganov, N. Hansen, Comput. Phys. Commun. 175 (2006) 713.